IV. CONCLUDING REMARKS

In the preceding sections we have developed a theory of the electronic ground state which is exact in two limiting cases: The case of a nearly constant density ($n=n_0+\tilde{n}(r)$, $\tilde{n}(r)/n_0 \ll 1$) and the case of a slowly varying density. Actual electronic systems do not belong to either of these two categories. The most promising formulation of the theory at present appears to be that obtained by partial summation of the gradient expansion (Sec. III.4). It has, however, not yet been tested in actual physical problems. But regardless of the outcome of this test, it is hoped that the considerations of this paper shed some new light on the problem of the inhomogeneous electron gas and may suggest further developments.

ACKNOWLEDGMENTS

This work was begun and, to a considerable extent, carried out at the University of Paris. One of the authors (P. Hohenberg) acknowledges with thanks a NATO Postdoctoral Fellowship; the other author (W. Kohn) a Guggenheim Fellowship. Both authors wish to thank the faculties of the École Normale Superieure, Paris, and the Service de Physique des Solides, Orsay, for their hospitality, and Professor A. Blandin, Professor J. Friedel, Dr. R. Balian, and Dr. C. De Dominicis for valuable discussions.

PHYSICAL REVIEW VOLUME 136, NUMBER 3B 9 NOVEMBER 1964

Scattering of a High-Intensity, Low-Frequency Electromagnetic Wave by an Unbound Electron*

ZOLTAN FRIED†
U. S. Naval Ordnance Laboratory, Silver Spring, Maryland and University of California, Santa Barbara, California

AND

JOSEPH H. EBERLY‡
U. S. Naval Ordnance Laboratory, Silver Spring, Maryland

(Received 15 June 1964)

"Thomson" scattering of a high-intensity, low-frequency, circularly-polarized electromagnetic wave by a free electron is considered. We find that by neglecting radiative corrections and pair effects, the Feynman-Dyson perturbation expansion is summable, and the sum can be analytically continued in the form of a sum of continued fractions. By imposing the boundary conditions that at $t=\pm\infty$ the photons and target electron propagate as free particles, we obtain results which differ from those reported by Brown and Kibble and by Goldman. In particular our results differ in two aspects. The first difference is in the kinematics; namely, we find no intensity-dependent frequency shift in the scattered photon. The second difference is in the dynamics; that is, we obtain a different expression for the scattering amplitude. Both of these changes originate in the choice of boundary conditions. Instead of treating the asymptotic radiation field classically, we choose our states as linear combinations of occupation-number states. Finally, contact is made with the results of Brown and Kibble and of Goldman using a mixed set of classical and quantum boundary values.

I. INTRODUCTION

THE advent of masers and lasers has stimulated a great deal of interest in the interaction of intense electromagnetic fields with matter. This activity has been focused on three different aspects of the subject. First, a great deal of attention has been devoted to the dynamics of production of high-intensity light.[1] A second area of concentration is the question of proper description of the electromagnetic radiation emanating from a laser; i.e., questions of coherence and correlation.[2] And finally, the problem of interaction of laser light with matter has attracted considerable interest.[3] It is this latter question to which we are devoting ourselves in this paper.

The particular problem of immediate interest is the effect of the presence of the high-intensity field on the Compton (Thomson) scattering amplitude. Recall that the Thomson amplitude describes the scattering of a

* A preliminary version of this work was presented at the Pasadena Meeting of the American Physical Society, Bull. Am. Phys. Soc. 8, 615 (1963).

† Present address: Lowell Technological Institute, Lowell, Massachusetts; on leave from the U. S. Naval Ordnance Laboratory.

‡ National Academy of Sciences—National Research Council Postdoctoral Research Associate, 1962–64.

[1] J. R. Singer, *Masers* (John Wiley & Sons, Inc., New York, 1900); F. Schwabl and W. Thirring (to be published); W. E. Lamb, Jr., Lecture Notes, Enrico Fermi International School of Physics, Varenna, 1963 (unpublished).

[2] R. Glauber, Phys. Rev. **130**, 2529 (1963); E. C. G. Sudarshan, Phys. Rev. Letters **10**, 277 (1963); E. Wolf, Proc. Phys. Soc. (London) **80**, 1269 (1962).

[3] J. A. Armstrong, N. Bloembergen, J. Ducuing, and P. S. Pershan, Phys. Rev. **127**, 1918 (1962); Z. Fried and W. M. Frank, Nuovo Cimento **27**, 218 (1963).

low-frequency photon by an unbound charged particle. From the point of view of photons the question of course is what, if any, effect does the presence of the other photons in the scattering region have on the probability amplitude for scattering of a single photon out of the incident beam. This question can be studied of course in perturbation theory.[4] One finds, however, that the results obtained in a power-series expansion diverge with decreasing ω (the angular frequency of the radiation). Since this divergency is a direct result of the photon's vanishing mass, it should perhaps be dubbed as the infrared divergence in the incident state.[5] Clearly, perturbation theory is misleading. It has been recognized by one of us (Z. F.) about a year ago that this divergence disappears when the problem is treated outside the context of perturbation theory.[6] The major defect of that treatment, however, is that only one part $(p\cdot A+A\cdot p)$ of the interaction Hamiltonian was included in the calculation. Subsequently, Brown and Kibble[7] and Goldman[8] have presented a more complete treatment including the $A\cdot A$ terms. They find: (a) that the scattering amplitude is modified in a nontrivial fashion by the presence of the external field, and (b) that there is a frequency shift in the scattered photon which is a function of the incident photon density. Their treatment is based essentially on the Volkov[9] solution of the Dirac equation in the presence of an external field.

The aim of this paper is twofold. On the one hand, we demonstrate that covariant perturbation theory yields summable results. Specifically, we show that the perturbation series can be summed, for sufficiently low values of the parameter $e^2\rho/m^2\omega$, in terms of infinite convergent continued fractions. The sum may then be analytically continued to arbitrarily high values of $e^2\rho/m^2\omega$. Consequently, this sum is no longer divergent as $\omega\rightarrow 0$. Also, we wish to stress that by using the Feynman-Dyson perturbation procedure and the adiabatic switching hypothesis, one finds that there is no intensity-dependent frequency shift in the scattered photon. The lack of frequency shift is a direct consequence of our way of treatment of this problem; viz., that asymptotically we describe the radiation field as a collection of freely propagating quanta. Another consequence of this choice of asymptotic states is that the scattering amplitude itself differs from the expressions found in Refs. 7 and 8. We will also show that with a certain set of asymptotic states the perturbation series reproduces the results of Brown and Kibble[7] and Goldman.[8]

In Sec. II we explain our method of summation, where for ease of presentation we consider a model theory with an interaction Lagrange density $L_I=g^2\phi^*(x)\phi(x)\chi^2(x)$. ϕ^* and ϕ are charged scalar fields whose quanta are massive particles. This is the target particle. $\chi(x)$ is a neutral scalar massless field whose quanta impinge on the target. The relative simplicity of this model is due to the fact that only one type of vertex appears in the calculation.

In Sec. III we consider electrodynamics, and to simplify the problem we treat the case of an incident beam of circularly polarized photons impinging on a spinless electron. The choice of scalar electrons does not greatly affect the results, since for low frequencies, spin effects are small. Here we content ourselves with leaving the answer expressed in continued fractions. The present state of the art in laser technology does not warrant a numerical evaluation of the answer.

In Sec. IV we apply our methods to harmonic production, while in Sec. V we attempt to elucidate the origin of the earlier results reported in the literature.[7,8]

Finally an Appendix concerning continued fractions and another on wave function normalization completes our discussion.

II. EXACT SEMICLASSICAL SOLUTIONS BY GRAPH SUMMATION

In this section we will show that certain so-called semiclassical problems may be solved exactly by summing all the Feynman graphs appearing in the perturbation series. (The precise meaning here of the term "semiclassical" will become apparent shortly.) Specifically, we solve exactly to all orders in the coupling constant, by graph summation, the problem of Compton scattering of a single spin-zero boson (called a ϕ particle) of mass μ by an intense beam of massless and spinless χ particles. That is, we are interested in the matrix element[10]

$$\langle p',k',(N-1)k\,|S|\,p,Nk\rangle \qquad \text{(II.1)}$$

in the limit that N, the number of χ particles in the beam, and V, the normalization volume, become very large, while the density of χ particles, $\rho=N/V$, remains finite and constant. Here $p_\mu=(E,\mathbf{p})$ and $p_\mu'=(E',\mathbf{p}')$ are the initial and final four-momenta of all χ particle; $k_\mu=(\omega,\mathbf{k})$ is the common four-momentum of all χ particles in the beam; and $k_\mu'=(\omega',\mathbf{k}')$ is the four-momentum of the single χ particle scattered out of the beam. These momenta describe the asymptotic ϕ and χ particles and so satisfy $p^2=p'^2=\mu^2$, and $k^2=k'^2=0$.

[4] Vachaspati, Phys. Rev. **128**, 664 (1962) and **130**, 2598(E) (1963); P. Stehle, J. Opt. Soc. Am. **53**, 1003 (1963).

[5] This infrared divergence is completely classical. See Vachaspati, Ref. 4.

[6] Z. Fried, Phys. Letters **3**, 349 (1963).

[7] L. S. Brown and T. W. B. Kibble, Phys. Rev. **133**, A705 (1964).

[8] I. I. Goldman, Phys. Letters **8**, 103 (1964).

[9] D. M. Volkov, Z. Physik **94**, 250 (1935).

[10] Strictly speaking, one should evaluate the S-matrix between so called coherent states. [These states of the radiation field are discussed by Glauber, Phys. Rev. **131**, 2766 (1963) and S. S. Schweber, J. Math. Phys. **3**, 831 (1962).] The transition amplitude (in the notation of Glauber) would then be a sum of terms

$$\sum_{N=1}^{\infty}\alpha_k{}^{*N-1}\alpha_k{}^N\langle p',(N-1)k,k'\,|S|\,p,Nk\rangle,$$

where $\alpha_k{}^N$ are arbitrary complex amplitudes. In the limit as $N\rightarrow\infty$, however, only one term survives.

Also, S is the scattering operator defined in the usual way[11] in terms of Dyson's time-ordering symbol T, and the normally ordered interaction Hamiltonian in the interaction picture $H_I(x)$:

$$S=1+\sum_{m\geq 1}\frac{(-i)^m}{m!}\int dx_1\cdots \times\int dx_m T[H_I(x_1)\cdots H_I(x_m)]. \quad \text{(II.2)}$$

In this model calculation we choose the interaction Hamiltonian to have the form

$$H_I(x)=+g^2N(\phi^*(x)\phi(x)\chi^2(x)), \quad \text{(II.3)}$$

where N indicates normal ordering, and $\phi(x)$ and $\chi(x)$ are the scalar field operators for the ϕ and χ particles, respectively. In the following sections, where we discuss electrodynamics, the χ particles will be given unit spin and H_I will acquire a linear term in accordance with gauge invariance, but the following method of summation will be seen to be able to accommodate these complications easily. Before embarking on the summation program we will introduce an important simplification which has the effect of defining what we mean by "semiclassical." We imagine the beam of χ particles to be very intense, and so ignore terms in the series (II.2) due to radiative corrections and virtual pair creation. Also we ignore processes in which more than one χ quantum is scattered from the incident beam.[12]

It is helpful at this point to make several observations about the Feynman graphs arising from the perturbation series. Each allowed graph consists of a single continuous ϕ particle line joined at a number of vertices by χ particle lines. The numbers of χ lines emitted and absorbed by the ϕ line are equal. All of the χ lines except one have momentum k_μ; the exception is an emission line with momentum k_μ'. For convenience we will refer to the vertex where this exceptional χ particle joins the ϕ line as the scattering vertex; all other vertices are forward-scattering, or, for short, nonscattering, vertices. The form of the interaction Hamiltonian makes it apparent that there are only two kinds of scattering vertex, and only three kinds of nonscattering vertex. These are illustrated in Figs. 1 and 2.

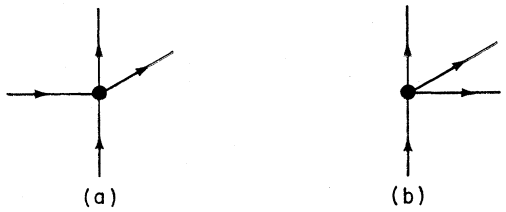

FIG. 1. Possible scattering vertices. The single vertical line is the ϕ particle, horizontal lines are the beam particles with momentum k_μ, and the skewed line is the scattered χ with momentum k_μ'. Incoming χ's are always drawn entering the diagram from the left; outgoing χ's leave the diagram to the right. The ϕ line is directed upward.

Let us look closely at a typical nonscattering vertex such as is shown in Fig. 3. The incoming virtual ϕ momentum is $p_\mu+2(m+1)k_\mu$, indicating that the ϕ particle has already absorbed a net number $2m+2$ of χ's from the beam. Application of the usual Feynman rules gives us the value of this vertex:

$$-i(2\pi)^4g^2(N-2m-1)^{1/2}(N-2m)^{1/2}/2\omega V,$$

where ω is the beam frequency and V is the normalization volume. The square-root factors come from the boson statistics involved in the double emission process; N is the very large number of χ's initially in the beam. In the limit $N,V\rightarrow\infty$, $N/V=\rho$, the vertex value becomes

$$-i(2\pi)^4g^2(\rho/2\omega). \quad \text{(II.4)}$$

By taking the limit at this stage we are implying that the beam density is so great that depletion effects are negligible. Consequently, all statistical factors become $\sqrt{N}$, so the value of any nonscattering vertex, whether it describes emissions or absorptions, is given by (II.4). The contribution of the propagators to the value of a graph is completely standard. The value of the propagator immediately following the vertex in Fig. 3 is

$$\frac{i}{(2\pi)^4}\frac{1}{(p+2mk)^2-\mu^2}=\frac{i}{(2\pi)^4}\frac{1}{4mp\cdot k}. \quad \text{(II.5)}$$

It is very convenient to adopt a simple condensed notation for the graphs. Observe that every graph has exactly the same number of nonscattering vertices as it has ϕ propagators. Starting at the bottom of a graph, each nonscattering vertex is associated with the propagator following it, until the scattering vertex is reached. It is not associated with any propagator. After the

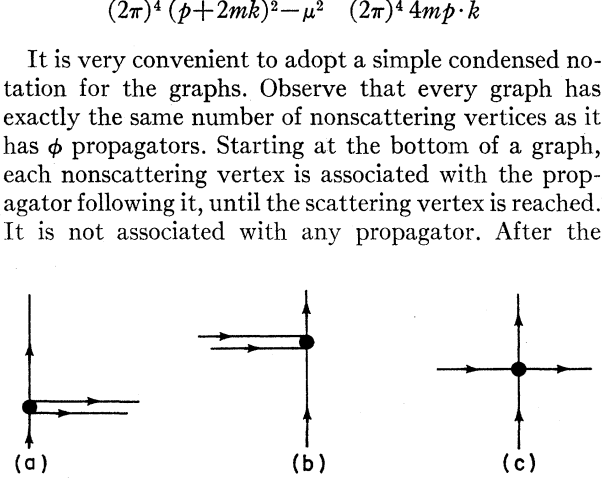

FIG. 2. Possible nonscattering vertices.

[11] Our factors of i and 2π, our choice of metric, and expressions which we refer to as "usual" or "familiar" will be those found in S. S. Schweber, *An Introduction to Relativistic Quantum Field Theory* (Row, Peterson Company, Evanston, Illinois, 1961).

[12] If the external field is large enough, then term by term an external field vertex will always contribute more to the amplitude than radiative corrections. If all the external vertex terms were positive, we could also state unequivocally that the sum total of radiative corrections is negligible. Since this is not the case we cannot conclude as to the effect of radiative corrections on the amplitude. In spite of this, it is still of great interest to study this incomplete problem. All the omissions made are of a nature which keeps the problem "classical"; i.e., all the parameters can be expressed in terms of classical quantities such as electromagnetic energy density, rest energy of the electron, and wave length of the incident light.

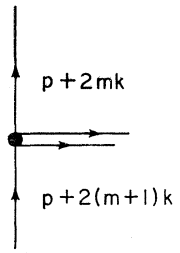

FIG. 3. A typical double-emission nonscattering vertex.

scattering vertex, each nonscattering vertex is associated with the propagator preceding it. The propagators and nonscattering vertices are thus paired in a simple and unambiguous way.

Then, since all vertices give the same contribution, we multiply each propagator value by the value of its associated vertex to get the propagator-vertex value appropriate to each segment of a graph. For example, the propagator-vertex value associated with the segment of the graph including the vertex and the propagator immediately following it in Fig. 3 is simply

$$x_{2m}=\frac{g^2\rho}{2\omega}\frac{1}{4mp\cdot k}\equiv\frac{\alpha}{2m}. \qquad \text{(II.6a)}$$

For the purposes of diagram summation the significant feature of the propagator-vertex factor x_{2m} is that it is proportional to $1/m$. For brevity we have lumped together the density dependence, the kinematic factors, and the $(p\cdot k)^{-1}$ term into a single proportionality constant $\alpha/2$. If the propagator-vertex pair under consideration occurs in the graph after the scattering vertex, we label the corresponding x factor with a prime to indicate this. Thus a typical segment following the scattering vertex, and after a net number $2m$ of χ's have been absorbed, would be denoted x'_{2m}, where the primed x's are the same as the unprimed ones except that p is replaced by p'. That is

$$x_{2m}'=\frac{g^2\rho}{2\omega}\frac{1}{4mp'\cdot k}=\frac{\alpha'}{2m}. \qquad \text{(II.6b)}$$

Only the value of the scattering vertex (which is not paired with a propagator) remains to be discussed. It is easy to see that both types of scattering vertex, Figs. 1(a) and 1(b) have the same value. By including into the value of the scattering vertex the kinematic factors for the initial and final free ϕ particles as well as the over-all four-momentum-conservation delta function for the entire graph, we obtain the following constant factor which appears in the value of every graph[13]:

$$-2ig(2\pi)^4\frac{\delta(p+k-p'-k')}{(16\omega\omega' EE')^{1/2}}\left(\frac{g^2\rho}{V^3}\right)^{1/2}. \qquad \text{(II.7)}$$

[13] The scattering vertex has an extra factor of $\sqrt{N}$ when the scattering is in the forward direction. This does not alter the angular distribution in the differential scattering cross section. For a clear exposition of this point, the reader is referred to Schwabl and Thirring (Ref. 1).

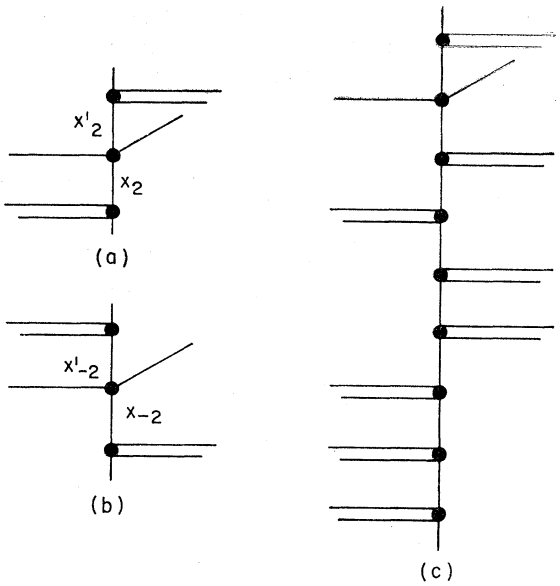

FIG. 4. Two low-order graphs and one higher order graph, all with a scattering vertex of the first kind.

Because the factor in (II.7) occurs in every graph we will ignore it in the summation and then tack it onto the final result.

Our method of attacking the graph summation will be to divide the graphs into several well-defined groups and sum the groups separately. To begin with, we temporarily exclude from consideration all graphs containing "straight-through" nonscattering vertices such as the one in Fig. 2(c). Since x_{2n} has not been defined for $n=0$, we also temporarily exclude all graphs containing x_0's. Then we consider the remaining graphs in this order: first those in which the scattering vertex is like that shown in Fig. 1(a) which we call type (a) graphs; and then those with scattering vertex like that in Fig. 1(b), which we call type (b) graphs.

Now we are ready to begin summing the type (a) graphs. To provide familiarity with the notation we explicitly evaluate the three graphs given in Fig. 4. The first two have the propagator-vertex factors keyed in. They have the values x_2x_2' and $x_{-2}x_{-2}'$, respectively. The last graph in Fig. 4 is of much higher order but is evaluated in the same way by assigning x factors to each propagator-vertex combination and multiplying them all together. Its value is $x_2(x_4x_2)^2(x_6x_4)x_2'$. Now notice that the value of any type (a) graph in which the scattering vertex immediately follows an x_2 graph segment may be written with its x factors similarly grouped. Every such graph consists, up to the scattering vertex, of an x_2 factor and pairs of x factors of the form $x_{2n}x_{2n-2}$; and after the scattering vertex consists of and pairs of x' factors of the form $x_{2m}'x_{2m-2}'$. The value of the general graph of the class may be written

$$x_2(x_4x_2)^{m_1}(x_6x_4)^{m_2}(x_8x_6)^{m_3}\cdots \times x_2'(x_4'x_2')^{l_1}(x_6'x_4')^{l_2}\cdots, \qquad \text{(II.8)}$$

that is, the general graph has m_1+1 segments with the value x_2, m_1+m_2 segments with the value x_4, and so on. To obtain the total contribution from all these graphs we sum over the m's and l's. However, first observe by comparing the graph in Fig. 5 with the high-order graph in Fig. 4 that several topologically distinct graphs may contribute the same value to the sum. We must therefore, before carrying out the m and l sums, multiply the general expression in (II.8) by an appropriate multiplicitly factor giving the number of different graphs with the same value (for given m's and l's). So our task is to count the numbers of different graphs with the same values. This is *easier* than it sounds. In the first place, without any x_4's in the graph there clearly cannot be any x_6's, and without x_6's, x_8's aren't possible, and so on. Also, at any x_2 segment an x_4 segment can be created simply by adding a two-χ absorption vertex such as in Fig. 2(b). But in order not to disturb the structure of the rest of the graph, a two-χ emission vertex must also be added immediately after the absorption vertex. This process is illustrated in Fig. 6. Thus, every time an x_4 is added, an x_2 is to be added immediately after it. Of course, this can be done any number of times in succession at any of the x_2 vertices in the graph. If it has been done once, then there is at least one x_4 in the graph, and by the same procedure one or any number of x_6x_4 pairs may be inserted into the x_4 segment. Thus we have the problem of counting the ways of putting indistinguishable factor pairs $x_{2m+2}x_{2m}$ into indistinguishable graph segments x_{2m}. This is easily solved. The number of ways to put k like marbles into n like boxes is given by the binomial coefficient $\binom{n+k-1}{k}$. Referring back to the general expression (II.8), we see we must multiply it by a product of binomial coefficients giving the number of ways to insert: m_2 pairs with the value x_6x_4 into m_1 segments labeled x_4; m_3 pairs with the value x_8x_6 into the m_2 segments labeled x_6, and so on. The same instructions obviously apply to the x''s separately from the x's; there is no way to mix them. Thus, we obtain the following expression:

$$x_2(x_4x_2)^{m_1}\binom{m_1+m_2-1}{m_2}(x_6x_4)^{m_2}\times\binom{m_2+m_3-1}{m_3}(x_8x_6)^{m_3}\cdots x_2'(x_4'x_2')^{l_1}\times\binom{l_1+l_2-1}{l_2}(x_6'x_4')^{l_2}\binom{l_2+l_3-1}{l_3}\cdots, \quad \text{(II.9)}$$

which is to be summed over all values of the m's and l's. The summations are most easily done in stages in a particular order. The method is demonstrated in Appendix A. The result is found to be expressible in terms of certain infinite continued fractions. In this first example, in which the type (a) scattering vertex occurs between the graph segments x_2 and x_2', the sum is given by

$$S_2^{(a)}=\frac{x_2}{1-F_2}\frac{x_2'}{1-F_2'}. \quad \text{(II.10)}$$

Here F_2 is a convergent continued fraction which is described in Appendix A. Explicitly, F_2 can be written

$$F_2=\cfrac{x_2x_4}{1-\cfrac{x_4x_6}{1-\cfrac{x_6x_8}{1-\cdot\\ \quad\cdot\\ \quad\quad\cdot}}}. \quad \text{(II.11)}$$

F_2' is the same as F_2 except that the x's are replaced by x''s.

Next we consider all those type (a) graphs whose scattering vertex follows an x_4 graph segment (two such graphs are illustrated in Fig. 7). The general graph

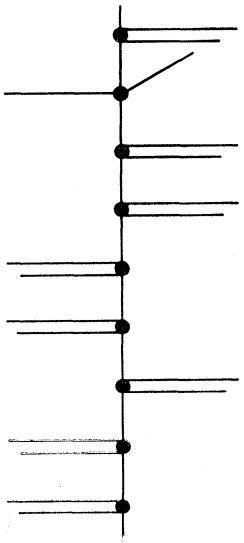

FIG. 5. Graph with different structure but same value as graph in Fig. 4(c).

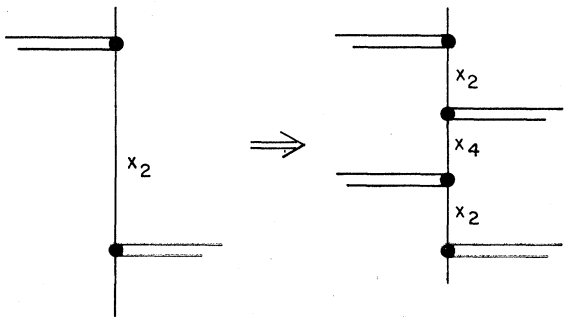

FIG. 6. The insertion of an x_4x_2 pair into an arbitrarily located x_2 segment.

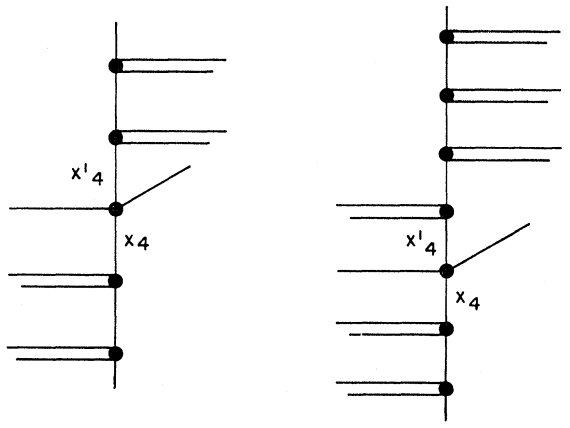

FIG. 7. Low-order graphs in which the scattering vertex lies between segments x_4 and x_4'.

value, with multiplicity factors included, is obtained by the same arguments that led to (II.9). It is

$$x_2x_4(x_4x_2)^{m_1}\binom{m_1+m_2}{m_2}(x_6x_4)^{m_2}\times\binom{m_2+m_3-1}{m_3}\cdots x_2'x_4'(x_4'x_2')^{l_1}\times\binom{l_1+l_2}{l_2}(x_6'x_4')^{l_2}\binom{l_2+l_3-1}{l_3}\cdots. \quad \text{(II.12)}$$

Note the slight difference in the multiplicity factors in (II.12) compared with (II.9). The difference is due to the fact that now all graphs must contain at least one x_4 and one x_4' factor as well as at least one x_2 and one x_2' factor. Again we must sum over all m's and l's, and again the result is a product of continued fractions:

$$S_4^{(a)}=\frac{x_2}{1-F_2}\frac{x_4}{1-F_4}\frac{x_2'}{1-F_2'}\frac{x_4'}{1-F_4'}. \quad \text{(II.13)}$$

Continuing in this fashion we easily determine, in terms of related continued fractions, the sums for all the graphs with scattering vertices like that in Fig. 1(a). If we denote by $S_{2m}^{(a)}$ the sum for all such graphs in which the type (a) scattering vertex lies between graph segments x_{2m} and x_{2m}', then we find

$$S_{2m}^{(a)}=\frac{x_2}{1-F_2}\cdots\frac{x_{2m}}{1-F_{2m}}\frac{x_2'}{1-F_2'}\cdots\frac{x_{2m}'}{1-F_{2m}'}. \quad \text{(II.14)}$$

It should be noted here that (II.14) holds for negative as well as positive values of m. A negative value of m merely signifies that the number of emissions prior to the scattering vertex exceeds the number of absorptions. From the original definition, Eq. (II.6a), we see that $x_{-m}=-x_m$; and since the F's are quadratic in the x's, $F_{-m}=F_m$. Thus, $S_{-2m}^{(a)}=S_{2m}^{(a)}$.

The contribution to the scattering amplitude from all allowed graphs having scattering vertex of type (a) is then the sum of all the S's:

$$A^{(a)}(\alpha,\alpha')\equiv\sum_{m=-\infty}^{\infty}S_{2m}^{(a)}, \quad \text{(II.15)}$$

where $S_0^{(a)}=1$, from the single lowest order graph (it cannot be modified without introducing x_0 factors, and so retains its unmodified value). Because of the connection between the S_{2m} and Bessel functions (explained in Appendix A), the final sum in Eq. (II.15) can actually be carried out in closed form:

$$A^{(a)}(\alpha,\alpha')=\frac{1}{J_0(\alpha)J_0(\alpha')}\sum_{-\infty}^{\infty}J_m(\alpha)J_m(\alpha')=\frac{J_0(\alpha-\alpha')}{J_0(\alpha)J_0(\alpha')}. \quad \text{(II.16)}$$

Next we consider all nonexcluded graphs in which the scattering vertex is like the one in Fig. 1(b). These will be referred to as graphs of type (b), and their contribution to the amplitude will be denoted $A^{(b)}(\alpha,\alpha')$. Again we will begin by summing all graphs which have an x_2 segment immediately prior to the scattering vertex. Momentum conservation at the scattering vertex then dictates that the segment following the scattering vertex should be x_0', which has been temporarily forbidden. Thus, when an x_2 segment immediately precedes scattering vertex (b), there can be no vertices following it. That is, the graphs look like those in Fig. 8. The value of any such graph may be written in a manner similar to Eq. (II.8), except that no x's appear. After including the proper multiplicity factors we find

$$S_2^{(b)}=\sum_{\{m\}}x_2(x_4x_2)^{m_1}\times\binom{m_1+m_2-1}{m_2}(x_6x_4)^{m_2}\cdots=\frac{x_2}{1-F_2},$$

where F_2 is the same continued fraction found earlier.

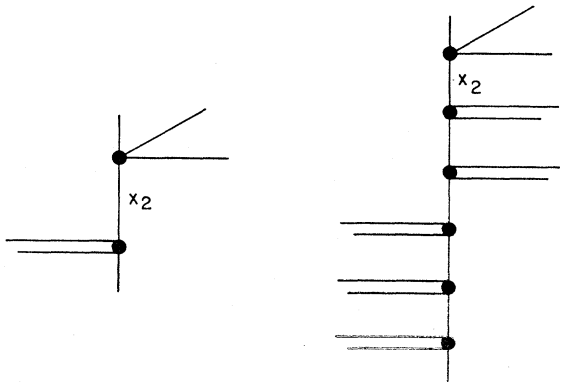

FIG. 8. No x' factors occur in graphs in which a double emission scattering vertex occurs immediately after an x_2 segment.

In general, for graphs of type (b), if the scattering vertex immediately follows an x_{2n} segment we find

$$S_{2n}{}^{(b)}(\alpha,\alpha')=\frac{x_2}{1-F_2}\cdots\frac{x_{2n}}{1-F_{2n}}\times\frac{x_2'}{1-F_2'}\cdots\frac{x_{2n-2}'}{1-F_{2n-2}'}. \quad \text{(II.17)}$$

Thus the contribution to the amplitude from graphs of type (b) is also easily found by adding all the $S_{2n}{}^{(b)}$:

$$A^{(b)}(\alpha,\alpha')=\sum_{-\infty}^{\infty}S_{2n}{}^{(b)}=\frac{J_1(\alpha-\alpha')}{J_0(\alpha)J_0(\alpha')}. \quad \text{(II.18)}$$

With the amplitude evaluated to this extent we return to the question of the excluded graphs. First we consider the graphs with one or more x_0's in them but still no straight-through interactions. Individually they are infinite; however, for each such graph it is possible also to draw its opposite—another graph equal in magnitude but with opposite sign. This is illustrated in two instances in Fig. 9, and may be proved rigorously. Because the graphs are individually infinite, the sums of the equal and opposite graphs must be examined in detail. The problem involved is essentially one of wave-function normalization, and can be handled in the usual way by explicitly introducing an adiabatic damping factor into the interaction Hamiltonian.[14] A more convenient method, for our purposes, which allows the summation of all such pairs of graphs in closed form is described in Appendix B. Of course both methods give the same result, which is to multiply $A(\alpha,\alpha')$ by the additional factor $J_0(\alpha)J_0(\alpha')$. Thus, to this point the wave-function-normalized amplitude $A_N(\alpha,\alpha')$, with the over-all factor of (II.7) included, is given by

$$-2ig^2\frac{(2\pi)^4\delta(p+k-p'-k')}{(16\omega\omega' EE')^{1/2}}\left(\frac{\rho}{V^3}\right)^{1/2}\times[J_0(\alpha-\alpha')+J_1(\alpha-\alpha')]. \quad \text{(II.19)}$$

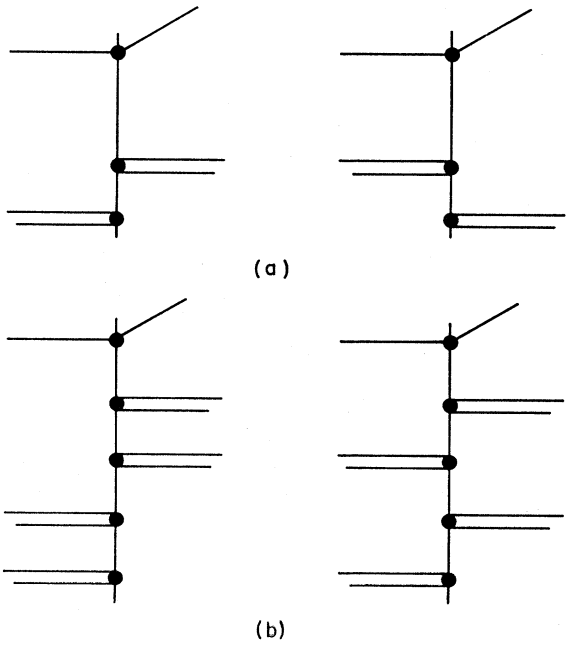

FIG. 9. Pairs of divergent graphs containing x_0 segments which when added together make finite contributions to the scattering amplitude.

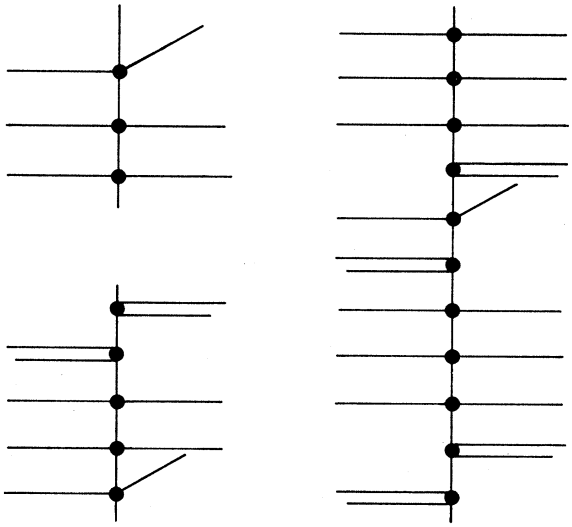

FIG. 10. Graphs with straight-through interactions in x_0 segments.

Next we include the straight-through lines, which can occur in any graph, by considering them in two classes. The first class consists of all graphs containing lines through x_0 segments; some such graphs are shown in Fig. 10. An involved but elementary calculation, which we omit, shows that the summation of all of these graphs only provides an over-all phase factor.[15] Thus they have no effect on the transition probabilities and we ignore them. The second class consists of all graphs with straight lines through any and all segments x_{2m}, where $m\neq 0$. This final modification is not quite straightforward and has significant effects; we will discuss it in some detail now.

Let us consider the addition of straight-through interactions in the same spirit as the foregoing developments. A straight-through interaction can be inserted into any segment x_{2m} without affecting in any way the ϕ momentum assignment at any propagator either before or after the insertion. The sole effect on the graph is to increase

[14] The technique is clearly detailed in Ref. 11, pp. 539–543.

[15] These graphs would normally lead to a mass shift for the electron due to its photon cloud. However, since we are ignoring radiative corrections, and since the external laser field is well localized, we have no such persistent effects. See, however, Sec. V.

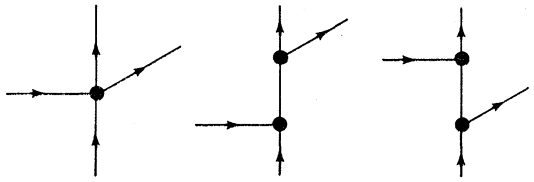

FIG. 11. Lowest order Compton scattering graphs. As before, the single vertical line is the electron, the horizontal lines are photons with wave vector k_μ, and the single skewed line is the scattered photon with wave vector k_μ'. Incoming (outgoing) photons are always drawn entering (leaving) the diagram from the left (to the right). All graphs satisfy $p_\mu+k_\mu=p_\mu'+k_\mu'$, where p_μ and p_μ' are the initial and final electron four-momenta.

by one the number of x_{2m} segments in it. Or, in other words, the x_{2m} into which the interaction was inserted becomes $(x_{2m})^2$. Clearly, this can be done any number of times in any segment. Thus, the entire effect of all such interactions is to make the replacement

$$x_{2n}\rightarrow\xi_{2n}=x_{2n}\sum_{l=0}^{\infty}(2x_{2n})^l=\frac{x_{2n}}{1-2x_{2n}}. \quad \text{(II.20)}$$

By returning to the original definition of the x's in Eqs. (II.6a), (II.6b) one observes that this inclusion of straight-through interactions is completely equivalent to a change in the ϕ mass:

$$\mu^2\rightarrow\mu^2+g^2\rho/\omega. \quad \text{(II.21)}$$

The effect on the amplitude of including the straight-through interactions is nontrivial. The replacement of x_{2m} by ξ_{2m} gives partial sums $S_{2m}{}^{(a)}$ and $S_{2m}{}^{(b)}$ which are again expressible as products of Bessel functions, but they are significantly more complicated than before. (The new continued fractions and their relation to Bessel functions are examined in Appendix A.) The wave-function-normalization factors are no longer simply $J_0(\alpha)J_0(\alpha')$.

The end result is that the fully normalized amplitude has the form

$$-2ig^2\frac{(2\pi)^4\delta(p+k-p'-k')}{(16\omega\omega'EE')^{1/2}}\left(\frac{\rho}{V^3}\right)^{1/2}\times[\mathcal{J}_0(\alpha,\alpha')+\mathcal{J}_1(\alpha,\alpha')], \quad \text{(II.22)}$$

where (with $\epsilon_0=1$, $\epsilon_{m\geqslant 1}=2$):

$$\mathcal{J}_0(x,y)=(N(x)N(y))^{-1/2}\times\left(\sum_{m\geqslant 0}\epsilon_m\frac{J_{-x+m}(x)J_{-y+m}(y)}{J_{-x}(x)J_{-y}(y)}+\begin{pmatrix}x\rightarrow -x\\ y\rightarrow -y\end{pmatrix}\right), \quad \text{(II.23)}$$

$$\mathcal{J}_1(x,y)=(N(x)N(y))^{-1/2}\times\left(\sum_{m\geqslant 1}\frac{J_{-x+m}(x)J_{-y+m-1}(y)}{J_{-x}(x)J_{-y}(y)}+\sum_{m\geqslant 0}\frac{J_{x+m}(-x)J_{y+m+1}(-y)}{J_x(-x)J_y(-y)}\right). \quad \text{(II.24)}$$

$N(x)$ is defined by the relation $\mathcal{J}_0(x,x)=1$.

With the inclusion of the straight-through interactions and the subsequent normalization, we have completed the summation of the semiclassical "Compton scattering" diagrams in our model. We now turn to electrodynamics.

III. ELECTRODYNAMICS AND COMPTON SCATTERING

We will apply to problems in electrodynamics the techniques described in the preceding section. The first such problem to be considered is that of Compton scattering in a high-intensity monochromatic laser beam of wave vector $k_\mu=(\omega,\mathbf{k})$. We will compute the scattering amplitude, as before, in the limit of large numbers of photons N, and volume V, such that the density ρ given by the ratio N/V remains fixed and finite. That is, we are interested in the S-matrix element

$$\lim_{\substack{N,V\rightarrow\infty\\ N/V=\rho}}\langle p';k',(N-1)k|S|p;Nk\rangle, \quad \text{(III.1)}$$

where $p_\mu=(E,\mathbf{p})$ and $p_\mu'=(E',\mathbf{p}')$ are the initial and final electron four-momenta, and $k_\mu'=(\omega',\mathbf{k}')$ is the wave vector of the scattered photon. These four-momenta satisfy $k^2=k'^2=0$, and $p^2=p'^2=M^2$, where M is the free-electron mass. In electrodynamics the interaction Hamiltonian $H_I(x)$ is somewhat more complicated than that used in the model calculation in the preceding section. It is given by the familiar expression

$$H_I(x)=+ieN(\phi^*\partial_\mu\phi-(\partial_\mu\phi^*)\phi)A^\mu-e^2N(\phi^*\phi A_\mu A^\mu). \quad \text{(III.2)}$$

We have, for simplicity, represented the electron by a scalar operator $\phi(x)$; $A_\mu(x)$ is the customary field operator for the electromagnetic potential.

The calculation of the exact scattering amplitude will be attacked in the same spirit as in the model calculation, by summing to all orders the Feynman graphs appearing in the perturbation series (II.2). The lowest order graphs are now three in number and are shown in Fig. 11. As in the model calculation of the preceding section, all higher order graphs will also consist of a single continuous electron line joined at a number of vertices by free photon lines. All of these photon lines except one are described by the beam wave vector k_μ; the odd photon has wave vector k_μ'. As before, we call the vertex where the odd photon joins the electron line

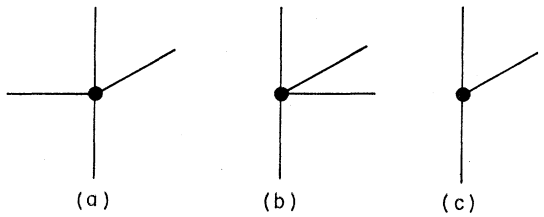

FIG. 12. Possible scattering vertices in scalar electrodynamics.

the scattering vertex; all others are nonscattering vertices. From the nature of the initial and final states of the S-matrix element of interest, Eq. (III.1), and from the structure of the interaction Hamiltonian given in Eq. (III.2), it is apparent that the nonscattering vertices consist of five kinds only. The terms in H_I which are linear in $A_\mu(x)$ give rise to vertices at which a single photon is either absorbed from or emitted into the beam; and the term in H_I which is quadratic in $A_\mu(x)$ leads to vertices at which two photon lines simultaneously meet the electron line. It is also easy to see that there are only three possible kinds of scattering vertex: two photons are simultaneously emitted with wave vectors k_μ and k_μ'; or, one photon with wave vector k_μ is absorbed from the beam and another with wave vector k_μ' is simultaneously emitted; or finally, a single photon is emitted with wave vector k_μ'. These varieties of scattering and nonscattering vertices are illustrated in Figs. 12 and 13.

As in the model calculation, we are able to make headway by dividing the possible combinations and mixtures of scattering and nonscattering vertices into several groups and then summing the groups of graphs separately. We chose to divide the graphs as follows. First, we temporarily exclude from consideration all graphs containing one or more electron propagators with vanishing denominators; we also temporarily exclude all nonscattering vertices arising from the quadratic term in H_I [that is, those vertices shown in Figs. 13(b) and 13(c)]. Then we consider the remaining graphs in this order: All graphs whose scattering vertex is similar to that shown in Fig. 12(a); then graphs with scattering vertex like that in Fig. 12(b); and finally graphs with scattering vertex like that in Fig. 12(c). These will be called graphs of types (a), (b), and (c), respectively.

Now, for the first set of graphs we proceed as follows. Except for the scattering vertex, each vertex can be paired with a propagator in the manner described in the model calculation. This gives rise to propagator-vertex factors for each segment of the graph, just as in the model calculation. Because the vertices are slightly different, the value of the typical factor will be different from the value in the model situation, but not in any unexpected way.

The value of the propagator-vertex factor x_n associated with the graph segments illustrated in Fig. 14 is determined from the usual Feynman rules for scalar electrodynamics in the manner described in the model

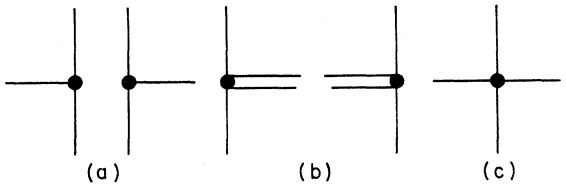

FIG. 13. Possible nonscattering vertices.

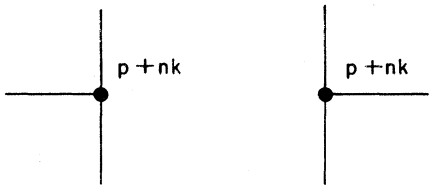

FIG. 14. Typical one-photon nonscattering vertices.

calculation. It is easily determined, in the limits $N,V\to\infty$, $N/V=\rho$, to be

$$x_n=\left(\frac{e^2\rho}{2\omega}\right)^{1/2}\frac{\epsilon\cdot p}{nk\cdot p}\equiv\frac{a}{n}, \tag{III.3a}$$

where $\epsilon=\epsilon_\mu(k)$, the polarization four-vector of a beam photon. As in the model calculation, if the graph segment falls after the scattering vertex we label the propagator-vertex factor with a prime:

$$x_n'=\left(\frac{e^2\rho}{2\omega}\right)^{1/2}\frac{\epsilon\cdot' p}{nk\cdot p'}\equiv\frac{a'}{n}. \tag{III.3b}$$

Due to the existence of two-photon as well as one-photon vertices in scalar electrodynamics, we must also compute the propagator-vertex factor y_n associated with graph segments of the types illustrated in Fig. 15. For our purposes only the value of 15(c) will be needed. In the limits $N,V\to\infty$ it is

$$y_m=\frac{e^2\rho}{2\omega}\frac{1}{mk\cdot p}\equiv\frac{b}{m}. \tag{III.4a}$$

We also label the y factors with a prime if the segment falls after the scattering vertex:

$$y_m'=\frac{e^2\rho}{2\omega}\frac{1}{mk\cdot p'}\equiv\frac{b'}{m}. \tag{III.4b}$$

Now we are in a familiar position; we can write down the value of any graph simply by writing the appropriate product of propagator-vertex factors and multiplying it by the constant over-all factor coming from the scattering vertex. In this case that over-all factor is easily found to be $+ieR_1\epsilon\cdot\epsilon'$, where

$$R_1=\frac{2(2\pi)^4\delta_{p+k,p'+k'}}{(16\omega\omega' EE')^{1/2}}\left(\frac{e^2\rho}{V^3}\right)^{1/2}, \tag{III.5}$$

and ϵ' means $\epsilon_\mu(k')$, the polarization vector for the scattered photon.

From this point everything goes exactly as in the model calculation. The type (a) summations give rise to products of infinite continued fractions; these in turn are related to Bessel functions; and ultimately all the summations can be performed explicitly. The result, to

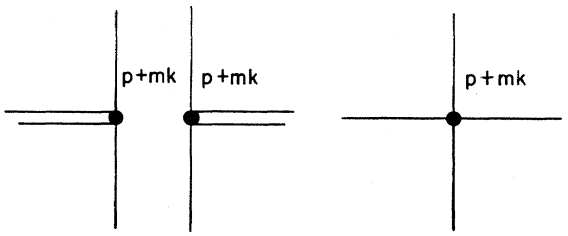

FIG. 15. Typical two-photon nonscattering vertices.

this stage of the calculation, is

$$+\mathrm{ie}R_1\frac{J_0(2a-2a')}{J_0(2a)J_0(2a')}\,\epsilon\cdot\epsilon'. \qquad \text{(III.6)}$$

Next we sum the set of type (b) graphs, those graphs in which the scattering vertex is like that in Fig. 12(b). The similarity to the model calculation is apparent here, too, and the result is

$$+ieR_1\frac{J_2(2a-2a')}{J_0(2a)J_0(2a')}\,\epsilon\cdot\epsilon'. \qquad \text{(III.7)}$$

However, the third set, those graphs with the scattering vertex like that in Fig. 12(c), is new and has no analog in the model. In the first place, the contribution of the scattering vertex itself is no longer a constant, but depends on its position in the particular graph under consideration. In a general graph, illustrated in Fig. 16, in which the scattering vertex occurs between the segments x_{n+1} and x_n', the contribution of the scattering vertex itself is $-ieR_2(p+(n+1)k)\cdot\epsilon'$, where

$$R_2=\frac{2(2\pi)^4\delta_{p+k,p'+k'}}{(8\omega'EE')^{1/2}}\frac{1}{V^{3/2}}. \qquad \text{(III.8)}$$

Also, by applying the rules for evaluating graphs and summing them we find the same continued fractions as before, but in slightly different combinations. It is straightforward to determine that the sum of this set of graphs is given by

$$ieR_2\sum_{n=-\infty}^{\infty}[p+(n+1)k]\cdot\epsilon'\left[\frac{J_{n+1}(2a)J_n(2a')}{J_0(2a)J_0(2a')}\right]. \qquad \text{(III.9)}$$

Here the required Bessel function summations are easily carried out using known identities[16] and an additional identity which may be derived easily:

$$(z/2)[J_0(z-z')+J_2(z-z')]=\sum_{m=-\infty}^{\infty}(m+1)J_{m+1}(z)J_m(z').$$

[16] G. N. Watson, *Theory of Bessel Functions* (Cambridge University Press, New York, 1958), p. 145.

After performing the sums, we obtain for this third set of graphs the result

$$ieR_2\left[\frac{J_1(2a-2a')}{J_0(2a)J_0(2a')}\right]\left(p\cdot\epsilon'+\frac{a}{a-a'}k\cdot\epsilon'\right). \qquad \text{(III.10)}$$

Now we may return to the excluded graphs. In just the same way as in the model problem we may explicitly include, in pairs, those graphs with zero denominators. By introducing adiabatic switching explicitly, the divergent terms are seen to cancel. The finite remainders again contribute with the net effect of multiplying the amplitude already obtained by the factor $J_0(2a)J_0(2a')$. Alternatively, as explained in Appendix B, we may regard the absence of these graphs from the sum as destroying the unitarity of the S matrix and leading to the necessity for wave function normalization. The normalization is easily carried out and leads to the same result. Thus, after adding the separate sums in Eqs. (III.6), (III.7), (III.10) and multiplying by $J_0(2a)J_0(2a')$, we have the gauge-invariant expression

$$-2ie\frac{(2\pi)^4\delta_{p+k,p'+k'}}{(16\omega\omega'EE')^{1/2}}\left(\frac{e^2\rho}{V^3}\right)^{1/2}\times[J_0(2a-2a')+J_2(2a-2a')]\times G_1, \qquad \text{(III.11)}$$

where G_1 is the gauge-invariant quantity given by

$$G_1=\epsilon\cdot\epsilon'+\frac{p\cdot\epsilon'\,p'\cdot\epsilon}{p'\cdot k}-\frac{p\cdot\epsilon\,p'\cdot\epsilon'}{p\cdot k}. \qquad \text{(III.12)}$$

Having summed all the diagrams with only one-photon nonscattering vertices [the type shown in Fig. 13(a)], we now go one step further and include two-photon nonscattering vertices. It is vastly simpler at this point to restrict the analysis to a circularly polarized laser beam. This choice will destroy the explicit gauge invariance we have maintained so far, but it also will allow us to ignore double-emission and double-absorption nonscattering vertices [shown in Fig. 13(c)]. This simplification is easily verified by expanding $A_\mu(x)A^\mu(x)$ in circular polarization operators, and using the fact that

$$\epsilon^R(k)\cdot\epsilon^R(k)=\epsilon^L(k)\cdot\epsilon^L(k)=0,$$

where $\epsilon^\lambda(k)$ is the polarization four-vector appropriate to a photon of wave vector k_μ and circular polarization λ. The only remaining two-photon nonscattering vertices for consideration are the straight-through variety

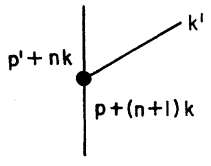

FIG. 16. Typical one-photon scattering vertex.

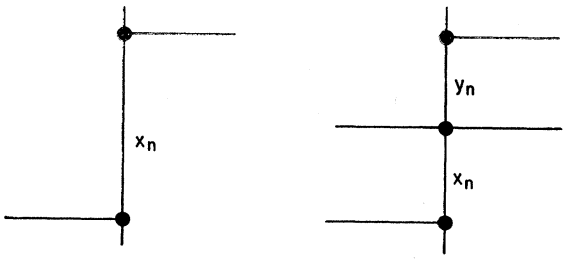

FIG. 17. Graph alteration due to the insertion of "straight-through" interactions.

[shown in Fig. 13(b)], and in the model calculation we have already indicated how they may be included with very little work.

The procedure for including the straight-through vertices is as follows. Into any graph segment, say one labeled x_m for definiteness, a straight-through interaction may be inserted as shown in Fig. 17. This makes two graph segments out of the original one, and changes the contribution to the graph value from x_m to $x_m y_m$. But there is no restriction on the number of times this process may be repeated. Adding a second straight-through vertex gives $x_m(y_m)^2$, and a third gives $x_m(y_m)^3$ for the value of the resulting segments. Just as in the model calculation, the net effect of adding an arbitrary number of straight-through vertices in every graph segment is to replace x_m by ξ_m, where now $\xi_m = x_m/(1-y_m)$. We can write ξ_m explicitly in terms of the constants a and b, and we obtain

$$\xi_m = \frac{2(e^2\rho/2\omega)^{1/2} p\cdot\epsilon}{(p+mk)^2 - M^2 - e^2\rho/\omega} = \frac{a}{m-b}, \quad \text{(III.13a)}$$

in the case of an absorption vertex, and

$$\xi_m^* = \frac{2(e^2\rho/2\omega)^{1/2} p\cdot\epsilon^*}{(p+mk)^2 - M^2 - e^2\rho/\omega} = \frac{a^*}{m-b}, \quad \text{(III.13b)}$$

for emission. The complex conjugates enter, of course, because of the decision to work with circular polarization states.

The replacement of x's by ξ's alters the form of the basic continued fractions almost exactly as it did in the calculations of Sec. II; and again the resulting covariant sums, the analogs of those in Eqs. (II.23) and (II.24), cannot be carried out. However, in this case we may simplify things considerably by completing the calculations in the laboratory reference system. This is because $p\cdot\epsilon = p\cdot\epsilon^* = 0$ if the electron is at rest. The resulting amplitude may be written

$$-2ie\frac{2(2\pi)^4\delta_{p+k-p'-k'}}{(16\omega\omega' EE')^{1/2}}\left(\frac{\rho}{V^3}\right)^{1/2} \times \mathfrak{N}[\epsilon\cdot\epsilon'^* + \Gamma\epsilon^*\cdot\epsilon'^*], \quad \text{(III.14)}$$

where $\mathfrak{N}$ is the normalization factor; also

$$\Gamma = e^{2i\phi'} J_{-b+2'}(2|a'|)/J_{-b'}(2|a'|)$$

and

$$\tan\phi' = \mathrm{Im}(a')/\mathrm{Re}(a').$$

The normalization factor $\mathfrak{N}$ is obtained in the same way as before (see Appendix B) and is found to be

$$\mathfrak{N}^{-2} = \tfrac{1}{2}\sum_{m=0}^{\infty}\epsilon_m\left[\frac{J_{-b'+m}(2|a'|)}{J_{-b'}(2|a'|)}\right]^2 + \{-b'\to b'\}. \quad \text{(III.15)}$$

IV. HARMONIC PRODUCTION

As we mentioned before, the number of photons present is so large that depletion of the beam due to a net absorption of 1, 2, or n photons from it cannot be expected to change the beam's characteristics in any important way. Thus one should expect, in the scattering of electrons in a laser beam, to find *all* of the (incoherent) processes which are represented by the matrix element:

$$\lim_{\substack{N,V\to\infty \\ N/V=\rho}} \langle p'; k', (N-n)k | S | p; Nk\rangle. \quad \text{(IV.1)}$$

When $n=1$ the matrix element of course describes Compton scattering; when $n>1$ it describes harmonic production at the harmonics of the beam frequency. The explicit calculation of the matrix element for any $n\geq 1$ presents no difficulties which have not already been discussed. We will discuss briefly the case $n\geq 1$, excluding for brevity the double-photon nonscattering vertices.

The graphs to be considered are graphs with $n-1$ more photons absorbed than emitted. Some low-order first harmonic graphs are illustrated in Fig. 18. Nonscattering vertices and electron propagators are again associated in the manner described earlier, so that each graph may easily be evaluated in terms of x factors. The graphs are again divided into groups according to the kind of scattering vertex and are summed first without including "straight-through" interactions or x_0's.

The general scattering vertex types which occur are labeled (a), (b), and (c), and are illustrated in Figs.

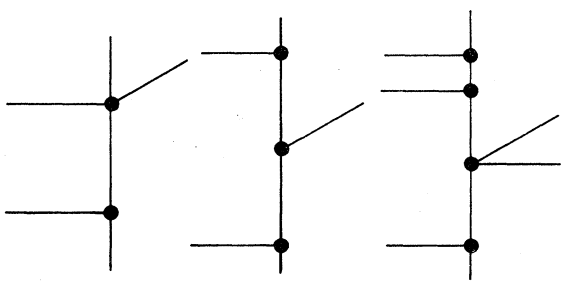

FIG. 18. Low-order graphs involved in first harmonic production. In all of the graphs $p+2k=p'+k'$.

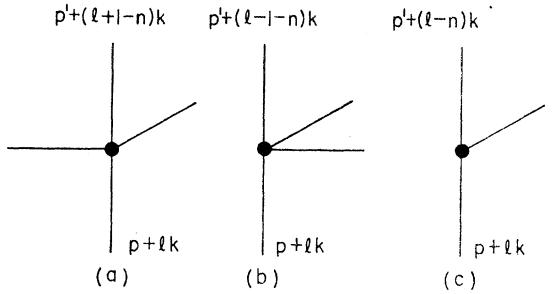

FIG. 19. The three types of scattering vertex for the $(n-1)st$ harmonic. In each graph $p+nk=p'+k'$.

19(a), (b), (c), respectively. In each case, immediately prior to the scattering vertex, the electron has momentum $p_\mu+lk_\mu$, having at that point absorbed a net number l of photons, where l can of course be any positive or negative integer. The momentum conservation relation for the $(n-1)$st harmonic, $p_\mu+nk_\mu=p_\mu'+k_\mu'$, then determines the momentum of the electron immediately following the scattering vertex. Following the earlier discussions in Secs. II and III one may directly write down the sums of all the graphs associated with each of the three scattering vertices for given values of n and l. One finds, after translating the continued fractions into Bessel functions,

$$J_l(2a)J_{l+1-n}(2a')/J_0(2a)J_0(2a'), \qquad \text{(IV.2a)}$$

$$J_l(2a)J_{l-1-n}(2a')/J_0(2a)J_0(2a'), \qquad \text{(IV.2b)}$$

$$J_l(2a)J_{l-n}(2a')/J_0(2a)J_0(2a'), \qquad \text{(IV.2c)}$$

for the sums of graphs associated with the scattering vertices of types (a) through (c), respectively.

It merely remains now to multiply each of Eq. (IV.2a)–(IV.2c) by the value of the appropriate scattering vertex and sum over all values of l. The vertex values for the general nth harmonic do not depend on n, and so are the same as given in the discussion of Compton scattering. The sums are easily performed using the Bessel function formulas already given. The normalization factor is also the same as in Compton scattering. So finally, after some simple rearrangement, the result of including everything in the sums except the straight-through interactions is found to be

$$\frac{-2ie(2\pi)^4\delta_{p+nk,p'+k'}}{(16\omega\omega' EE')^{1/2}}\left(\frac{e^2\rho}{V^3}\right)^{1/2} \times[J_{n-1}(2a-2a')+J_{n+1}(2a-2a')]\times G_n. \qquad \text{(IV.3)}$$

This is seen to be almost identical with the comparable expression, Eq. (III.11), obtained for Compton scattering. The sole differences are the change in the Bessel function indices and the simple generalization from the gauge-covariant product $G_1\delta_{p+k,p'+k'}$ to the gauge-covariant quantity $G_n\delta_{p+nk,p'+k'}$, where G_n is

$$G_n=\epsilon\cdot\epsilon'+\frac{p\cdot\epsilon'\ p'\cdot\epsilon}{nk\cdot p'}-\frac{p\cdot\epsilon\ p'\cdot\epsilon'}{nk\cdot p}. \qquad \text{(IV.4)}$$

The consideration of the remaining (two-photon) vertices has the same complicating effect on the amplitude (IV.3) as on the Compton scattering amplitude (III.11). Since it would add nothing new to the discussion, we will not explicitly write out the resulting complete amplitude for harmonic production.

We may point out here a consequence of the fact that we have ignored the spin of the electron. Notice that because $J_m(0)=\delta_{m0}$, Eq. (IV.3) says that harmonic production in the forward direction (where $a=a'$) vanishes. This is easily understood, since the total spin of n incoming photons with frequency ω cannot be carried away by the single forward-scattered photon with frequency $n\omega$ if $n>1$. If the electron were given spin, however, forward scattering in the first harmonic only would also be possible, since the electron by reversing its spin could carry off one extra unit of angular momentum.

V. DISCUSSION AND CONCLUSIONS

It remains for us to compare our results with those found in Refs. 7 and 8, and to comment on the origin of the differences obtained. In particular, we must indicate why we find no intensity-dependent frequency shift in the scattered photon, and also why our amplitude differs.

The answer to the first question is implicit in our treatment of the problem. We compute the transition amplitude for a scattering event in which one and only one photon is removed from the incident beam. Hence, if there were initially N photons in state k, then in the final state $N-1$ photons will occupy state k. Since the S matrix commutes with the momentum (energy) operator we immediately have

$$p_\mu+Nk_\mu=p_\mu'+(N-1)k_\mu+k_\mu' \qquad \text{(V.1)}$$

or

$$p_\mu+k_\mu=p_\mu'+k_\mu',$$

where p, p' are the initial and final momenta of the target electron and k' is the momentum of the scattered photon. The above equality is of course independent of N. Hence, we obtain no intensity-dependent frequency shift. Furthermore, this analysis remains valid even if we describe the incident and final states of the radiation field in terms of "coherent" states.[10] In that case the incident and final states are

$$|\Phi_i\rangle=\sum_{N=1}^{\infty}\alpha_N(k)|Nk,p\rangle;$$

$$|\Phi_f\rangle=\sum_{N=0}^{\infty}\alpha_N(k)|Nk,k',p'\rangle, \qquad \text{(V.2)}$$

respectively. The S-matrix element is given by

$$\langle\Phi_f|S|\Phi_i\rangle=\langle\Phi_f|\Phi_i\rangle + \sum_{N=1}^{\infty}\alpha_N\beta^*_{N-1}\langle(N-1)k,k',p'|S-1|p,Nk\rangle. \quad (V.3)$$

Since the states $|p,Nk\rangle$ are eigenstates of the total momentum operator P_μ, and $[S,P_\mu]=0$, Eq. (V.2) may be rewritten as

$$\langle\Phi_f|S|\Phi_i\rangle=\langle\Phi_f|\Phi_i\rangle+i(2\pi)^4\delta(p+k-p'-k') \times\sum_{N=1}\alpha_N\beta^*_{N-1}\langle(N-1)k,k',p'|T|p,Nk\rangle. \quad (V.4)$$

In obtaining the right-hand side of Eq. (V.4) we make no use of perturbation theory. Our only assumption is that asymptotically, i.e., at $t=\pm\infty$, the electron and photons do not interact. We also note that the argument of the function does not depend on N. The only dependence on N is in the T-matrix element. It is only at this stage, in the computation of the T-matrix element, that we pass to the "classical" limit in the sense that any depletion or enhancement effects due to the Bose-Einstein statistics are ignored: Any factor of the form $\sqrt{(N\pm m)}$ is replaced by $\sqrt{N}$ in the limit as $N\to\infty$.

In contrast to this, the treatment given in the literature[7,8] is, as far as the radiation field is concerned, *ab ovo* classical. Hence after switching on the external field the electron can absorb and emit radiation in a completely continuous fashion. Similarly, the energy of the external field can be shared in a continuous way between the electron the incident radiation mode and the scattered radiation mode. Thus there is no counterpart to Eqs. (V.1) and (V.4), and an intensity-dependent frequency shift cannot be ruled out on purely classical arguments. Indeed, as shown by Brown and Kibble[7] and Goldman,[8] such frequency shifts appear.

Interestingly enough, we can, after suitable manipulation, also obtain such results. Briefly, we split the interaction Hamiltonian density, Eq. (III.2), into two parts

$$H_I(x)=H_I^{(1)}(x)+H_I^{(2)}(x), \quad (V.5)$$

where

$$H_I^{(1)}(x)=ieN\{\phi^*\overleftrightarrow{\partial_\mu}\phi\}A^\mu - e^2N\{\phi^*\phi(A_\mu^{(+)}A^{\mu(+)}+A_\mu^{(-)}A^{\mu(-)}\}, \quad (V.6)$$

and

$$H_I^{(2)}(x)=-e^2N\{\phi^*\phi(A_\mu^{(+)}A^{\mu(-)}+A_\mu^{(-)}A^{\mu(+)})\}. \quad (V.7)$$

By replacing $H_I^{(2)}(x)$ by its c-number value and incorporating it with $H_0(x)$ of the electron field, one obtains a new momentum energy relationship for the electron:

$$\bar{p}^2=m^2+\Delta m^2=m^2+e^2\rho/\omega. \quad (V.8)$$

Following Brown and Kibble we set

$$\bar{p}=p+\Delta m^2(2p\cdot k)^{-1}k;\quad \bar{p}'=p'+\Delta m^2(2p'\cdot k)^{-1}k. \quad (V.9)$$

And now upon evaluating

$$\lim N\to\infty,\ V\to\infty\langle\bar{p}',(N-1)k,k'|\bar{S}|\bar{p},Nk\rangle,$$

where the perturbation series for $\bar{S}$ contains only $H^{(1)}$ and not $H^{(2)}$, we obtain agreement (in the case of scalar electrons) with Brown and Kibble[7] and Goldman.[8] Of course the frequency shift follows now simply from the standard Compton relations with $\bar{p}$ and $\bar{p}'$ replacing p and p':

$$\bar{p}_\mu+k_\mu=\bar{p}_\mu'+k_\mu'. \quad (V.10)$$

To recapitulate, agreement with Refs. 7 and 8 can be obtained both as regards the frequency shift and the scattering amplitude within the context of perturbation theory, but only at the expense of choosing asymptotic states for the electron which do not represent free particles.

Note added in proof. It should be pointed out that if one were to subject our results to empirical verification, the experimental setup would have to be such as to satisfy the assumption that the passage time of the laser pulse past the target electron is of relatively short duration. That is to say, by the time the scattered photon is detected, the target electron 'sees' no more photons. Only then can we insist that the outgoing state for the target describes a free-particle state. (Notice that such considerations are not necessary for standard two-particle scattering problems.) If, however, the passage time of the laser beam past the target electron is of such a large duration that we can start detecting scattered photons while the target electron is still interacting with the rest of the photons in the 'coherent' beam, then we are faced with a problem which differs fundamentally from standard scattering problems. [See in this connection M. L. Goldberger and K. M. Watson, Phys. Rev. **134**, B919 (1964) and references therein.]

It is somewhat surprising that a classical treatment of the radiation field with correct asymptotic values for the electron propagation should yield identical results with a quantum treatment of the radiation field and asymptotically altered electron states. This does point out, however, that our differing scattering amplitude is a direct result of the lack of frequency shift. Within the framework of the Feynman-Dyson perturbation procedure, the two differing scattering amplitudes correspond to solving the differential equation for the U matrix with different boundary conditions.

Finally, we wish to allay any misgivings about the use of perturbation theory by noting that the use of Dyson's U matrix in which $H_I(t)$ is replaced by $e^{-\alpha|t|}H_I(t)$ is eminently suitable for this type of problem. Since self-fields are ignored and only external fields of limited space-time extent are considered, the factor $e^{-\alpha|t|}$ automatically accomplishes the asymptotic separation of the electron from the laser beam.

ACKNOWLEDGMENTS

We are grateful to Dr. W. M. Frank, Dr. L. S. Brown, Dr. P. J. Redmond, and Dr. H. Ezawa for helpful com-

ments, and to Dr. Z. I. Slawsky for continued interest in this work. We particularly thank Dr. Redmond for pointing out a mistake concerning the circularly polarized case in the original manuscript.

APPENDIX A: CONTINUED FRACTIONS

In the text in Eq. (II.15) the scattering amplitude is written as a sum of products of continued fractions. The calculation of the first term in the sum $S_2^{(a)}$ is typical of the other S_{2m} and will be described in this appendix. Additionally we will mention some of the pertinent analytic properties of the continued fractions, and conclude from them that the formal manipulations involving continued fractions implied in the text may be performed rigorously.

Recall that $S_2^{(a)}$ was defined to be the sum over all m's and l's from 0 to ∞ of the general graph value given in Eq. (II.9). That is,

$$S_2=\sum_{\{m\}} x_2(x_4x_2)^{m_1}\binom{m_1+m_2-1}{m_2}(x_6x_4)^{m_2}$$
$$\binom{m_2+m_3-1}{m_3}(x_8x_6)^{m_3}\cdots\sum_{\{l\}} x_2'(x_4'x_2')^{l_1}$$
$$\times\binom{l_1+l_2-1}{l_2}(x_6'x_4')^{l_2}\binom{l_2+l_3-1}{l_3}(x_8'x_6')^{l_3}\cdots. \quad \text{(A1)}$$

Clearly, the m and l sums are independent and may be done separately. Denote them by M and L, respectively, so that $S_2^{(a)}=M\times L$ and consider M first. Obviously a subset among the set of graphs which sum to S_2 comprises those graphs which have only x_2 and x_4 segments in them. The contribution of these graphs to M is easily computed by setting $m_2=m_3=m_4=\cdots=0$ and performing the sum over m_1. Call the contribution of the subset M_4; then one finds, assuming α is small enough so that the x's are small and the series converges,

$$M_4=x_2/(1-x_2x_4). \quad \text{(A2)}$$

A larger subset which contains the M_4 subset is the set of all graphs which have only x_2, x_4, and x_6 segments in them. The contribution of this subset to M, denoted M_6, is also easily computed. Set $m_3=m_4=m_5=\cdots=0$, and sum first over m_2, then m_1. One finds, again assuming small enough α,

$$M_6=\cfrac{x_2}{1-\cfrac{x_2x_4}{1-x_4x_6}}. \quad \text{(A3)}$$

By continuing this procedure to larger and larger subsets of the whole, one is rapidly convinced that the pattern is generally true. A proof by induction is then simple to construct in order to establish rigorously that, for any integer $2n$, the contribution to M made by those graphs with only $x_2, x_4,\cdots,x_{2n}$ segments in them is

$$M_{2n}=\cfrac{x_2}{1-\cfrac{x_2x_4}{1-\cfrac{x_4x_6}{1-\cdot\\ \quad\cdot\\ \quad\cdot\\ \quad\cfrac{}{1-x_{2n-2}x_{2n}}}}}. \quad \text{(A4)}$$

The quantity of interest is, of course, $M=\lim_{n\to\infty} M_{2n}$. One can establish that the infinite continued fraction[17] obtained in the limit exists as a well-behaved function of α. In fact, with the aid of theorems due to Van Vleck,[18] it can be shown not just that the continued fraction converges for sufficiently small α, but that it converges to a meromorphic function of α which is regular at $\alpha=0$. Even more, the convergence is uniform throughout the *entire finite α plane* away from the isolated poles of the function. Thus the sum M may be written as a convergent continued fraction which analytically continues the power series from its region of convergence near the origin into the entire finite α plane. Since α is directly proportional to the density ρ, it is by means of this analytic continuation that one is able to evaluate the Feynman perturbation series outside of its region of convergence.

It is evident that there is no essential difference between the summation and limit leading to M and the one leading to L. Thus, the results of the preceding paragraphs may be taken over bodily to evaluate L in terms of a continued fraction. The result for L is the same as for M except that α is replaced by α'.

The continued fractions obtained here are well known in classical analysis. It can be shown[18] that

$$x_2/(1-F_2)=J_1(\alpha)/J_0(\alpha), \quad \text{(A5)}$$

and more generally that

$$x_{2m}/(1-F_{2m})=J_m(\alpha)/J_{m-1}(\alpha),$$

where $J_m(\alpha)$ is the usual cylindrical Bessel function of the first kind, and where F_{2m} is defined by the recursion relation

$$F_{2m}=x_{2m}x_{2m+2}/(1-F_{2m+2}), \quad \text{(A6)}$$

and the boundary condition $F_{2m}=0(\alpha^2)$ as $\alpha\to 0$.

Matters become more complicated when the straight-through interactions of the text force the replacement of

[17] That the result of the summation should be expressible as a continued fraction is not surprising in light of the close similarity of our procedure and that of the Feenberg perturbation theory (cf. P. M. Morse and H. Feshbach, *Methods of Theoretical Physics* (McGraw-Hill Book Company, Inc., New York, 1953), Vol. II, pp. 1010-1018.

[18] Cf. H. S. Wall, *Continued Fractions* (D. Van Nostrand and Company, Inc., New York, 1948).

x_{2m} by ξ_{2m}. Now the fractions, written $\mathfrak{F}_{2m}$ are defined by the recursion formula

$$\mathfrak{F}_{2m}=\xi_{2m}\xi_{2m+2}/(1-\mathfrak{F}_{2m+2}), \tag{A7}$$

with the same boundary condition. These $\mathfrak{F}$'s are less straight forward to analyze because ξ_{2m} is not proportional to $1/2m$ as x_{2m} was. However, Wall[18] shows that they are still related to Bessel functions. We may write

$$\frac{\xi_{2m}}{1-\mathfrak{F}_{2m}}=\frac{J_{m-\alpha}(\alpha)}{J_{m-1-\alpha}(\alpha)} \tag{A8}$$

and this is the form we have employed to express the complete amplitudes in Eqs. (II.22), (II.23) and (III.14), (III.15).

APPENDIX B: WAVE-FUNCTION RENORMALIZATION

To complete our computational program, we have to account for all the graphs excluded up to the present point. We are of course interested in evaluating the matrix-element $\langle p',(N-1)k,k'|S|p,Nk\rangle$ as a power-series expansion in the limit as $N\to\infty$. Some of the expansion coefficients refer to transitions which proceed via the initial state. This is characteristic of perturbation theory in general. In the case of a discrete spectrum, these transitions give rise to vanishing denominators, which cannot be computed in a direct manner. In nonrelativistic (noncovariant) stationary state perturbation theory the algorithm for calculating these coefficients is well known.[19] We shall, nevertheless, recapitulate it here in order to bring out the similarity of our procedure to that employed in noncovariant stationary state perturbation theory. Briefly, one is given a Hamiltonian $H=H_0+H_I$, and the spectrum and the state vectors of H_0, viz., $H_0|n\rangle=\epsilon_n|n\rangle$. The state vector $|\Phi_i\rangle$ which is an eigenstate of H_0+H_I can now be computed to be: $|\Phi_i\rangle=\sum_n a_n^{(i)}|n\rangle$. The computation of the $a_n^{(i)}$ is done in two steps. First, one computes $\tilde{a}_n^{(i)}$, where $\sim$ denotes the instruction that all terms with one or more vanishing denominators are to be omitted from the calculation. Next, by making use of the normalization requirement $\langle\Phi_i|\Phi_i\rangle=1$, one obtains

$$a_n^{(i)}=\tilde{a}_n^{(i)}\Big(1+\sum_{m\neq i}|\tilde{a}_m^{(i)}|^2\Big)^{-1/2}.$$

Our procedure, aside from some necessary modifications, is similar. To make our discussion as transparent as possible, it will help to recall that in the scattering matrix element of interest the nonforward scattering line occurs at one vertex only. This observation allows us a convenient way to separate the interacting part of the Hamiltonian as follows: We write H_I of the model problem [Eq. (II.3)] in the interaction picture as

$$H_I=\hat{H}+\lambda h|_{\lambda=g},$$

where

$$\hat{H}=g\int\phi^*(x)\phi(x)[\chi_k^{(+)}e^{ik\cdot x}+\chi_k^{(-)}e^{-ik\cdot x}]^2d^3x \tag{B1}$$

and

$$h=\int\phi^*(x)\phi(x)[\chi^2(x)-(\chi_k^{(+)}e^{ik\cdot x}+\chi_k^{(-)}e^{-ik\cdot x})^2]d^3x.$$

According to Dyson, the S-matrix element can be written as

$$\langle p',(N-1)k,k'|S|p,Nk\rangle=\langle p',(N-1)k,k'|$$
$$\times P\exp\Big\{-i\int[\hat{H}(t)+\lambda h(t)]dt\Big\}|p,Nk\rangle\Big|_{\lambda=g}. \tag{B2}$$

Since our computations are to first order in λ (and to all orders in $\hat{H}$), it is convenient to rewrite Eq. (B2) as

$$\langle p',(N-1)k,k'|S-1|p,Nk\rangle=\frac{\partial}{\partial\lambda}g\langle p',(N-1)k,k'|P\exp\Big\{-i\int[\hat{H}(t)+\lambda h(t)]dt\Big\}|p,Nk\rangle\Big|_{\lambda=0}. \tag{B2'}$$

Furthermore,

$$\frac{\partial}{\partial\lambda}g\langle p',(N-1)k,k'|P\exp\Big\{-i\int[\hat{H}(t)+\lambda h(t)]dt\Big\}|p,Nk\rangle\Big|_{\lambda=0}$$
$$-i=g\langle p',(N-1)k,k'|P\exp\Big[-i\int_0^\infty\hat{H}(t)dt\Big]\int_{-\infty}^{\infty}h(t')dt'P\exp\Big[-i\int_{-\infty}^0\hat{H}(t)dt\Big]|p,Nk\rangle$$
$$-i=g\langle p',(N-1)k,k'|\hat{U}^{-1}(0,+\infty)\int_{-\infty}^{\infty}h(t')dt'\hat{U}(0,-\infty)|p,Nk\rangle, \tag{B3}$$

[19] L. I. Schiff, *Quantum Mechanics* (McGraw-Hill Book Company, Inc., New York, 1955), p. 152–154.

where

$$\hat{U}(0,-\infty)=P\exp\left[-i\int_{-\infty}^{0}\hat{H}(t')dt'\right]$$

and

$$\hat{U}^{-1}(0,+\infty)=P\exp\left[-i\int_{0}^{\infty}\hat{H}(t')dt'\right].$$

This equality can be most easily ascertained by expanding both sides of Eq. (B3).

In passing we wish to point out that at this stage wave-function renormalization can be carried out by simply writing

$$\hat{U}(0,-\infty)|p,Nk\rangle=\frac{\hat{U}'(0,-\infty)|p,Nk\rangle}{(\langle p,Nk|\hat{U}'^{\dagger}(0,-\infty)\hat{U}'(0,-\infty)|p,Nk\rangle)^{1/2}},\tag{B4}$$

where the prime is a shorthand notation for the perturbation development of the $\hat{U}$ matrix in which vanishing energy denominators have been excluded. However, such a task is arduous and is fundamentally noncovariant.

We now come to the crucial part of our wave-function renormalization method. Since $\hat{H}$ is that part of the interacting Hamiltonian which contains no radiative corrections or pair effects, we obtain an important identity, viz.

$$\hat{U}(0,+\infty)|p,Nk\rangle=\hat{U}(0,-\infty)|p,Nk\rangle.\tag{B5}$$

This identity can be established by expanding both sides in a power series. Performing the integrations we note that the lower limit on the integrals play no essential role. The only place where the damping factor from the infinite limits of integration enters the scene is when a transition occurs back to the initial state. Since the intermediate states entering into the expansion are, for fixed p_μ, discrete in character (i.e., $|m\rangle=|p_m,mk\rangle$; $H_0|m\rangle=(p_0+mk_0)|m\rangle$), the sign of the damping factor is immaterial.

With the aid of Eq. (B5) one obtains

$$g(\partial/\partial\lambda)\langle p',(N-1)k,k'|P\exp\left\{-i\int[\hat{H}(t)+\lambda h(t)]dt\right\}|p,Nk\rangle\Big|_{\lambda=0}$$
$$=-ig\langle p',(N-1)k,k'|\hat{U}^{-1}(0,+\infty)\int_{-\infty}^{\infty}h(t')dt'\hat{U}(0,+\infty)|p,Nk\rangle.\tag{B6}$$

In the limit of forward scattering $p'\to p$, $k'\to k$ and the S-matrix element is now equal to

$$\langle p,Nk|S-1|p,Nk\rangle=F(p,k)\langle p,Nk|$$
$$\times\hat{U}^{-1}(0,+\infty)\hat{U}(0,+\infty)|p,Nk\rangle=F(p,k).\tag{B7}$$

The meaning of Eq. (B7) is simply that the covariant forward scattering S-matrix element is equal to the normalization of the incident state times some factor. So the task of normalization of the incoming (or outgoing) state consists of factoring a part of the S-matrix expansion in which the scattering occurs. Although this can be done, the procedure as it stands is still cumbersome.

At this stage, however, one can easily resort to a trick which will facilitate the task. Introduce a new Hamiltonian

$$H'=H+H_0'+\eta H_I',\tag{B8}$$

where H is the same as the model Hamiltonian of Sec. II, H_0' is the kinetic energy part of the Hamiltonian appropriate to a new scalar field $\xi(x)$. This new field interacts only with $\phi(x)$ through the interaction Hamiltonian

$$H_I'=\int\phi^*(x)\phi(x)\xi^2(x)d^3x.$$

The S-matrix element for the scattering of a single ξ quantum off the target particle (ϕ quantum) in the presence of N particles of the χ field is given by

$$\langle p',Nk,q'|S|p,Nk,q\rangle=\langle p',Nk,q'|P$$
$$\times\exp\left[-i\int(H_I+\eta H_I')dt\right]|p,Nk,q\rangle,\tag{B9}$$

where

$$|p,Nk,q\rangle=\xi_q^{(-)}|p,Nk\rangle,\tag{B10}$$
$$|p',Nk,q'\rangle=\xi_{q'}^{(-)}|p',Nk\rangle,$$

and $|p,Nk\rangle$, $|p',Nk\rangle$ are eigenstates of H_0 (model) as before. If we again neglect radiative corrections and

pair effects, then Eq. (B9) is simply

$$\langle p',Nk,q'|S-1|p,Nk,q\rangle=i\langle p',Nk|\xi_{q'}{}^{(-)}$$
$$\times\hat{U}(0,\infty)\eta\int_{-\infty}^{\infty}H_I'dt\,\hat{U}(0,\infty)\xi_q{}^{(+)}|p,Nk\rangle, \quad \text{(B11)}$$

which in the limit of forward scattering is

$$\langle p,Nkq|S'-1|p,Nk,q\rangle=2i\eta(2\pi)^4$$
$$\times(16q_0{}^2EE'V^3)^{-1/2}\langle p,Nk|$$
$$\times\hat{U}'^{\dagger}(0,+\infty)\hat{U}'(0,+\infty)|p,Nk\rangle; \quad \text{(B12)}$$

where the primes have been added to indicate that the equality holds also when vanishing denominators are omitted from the calculation.

The simplicity of factorization in the latter method stems from: (i) It is easy to identify the scattering vertex by virtue of the fact that it consists of a line depicting a different particle, and (ii) that there is only one type of vertex, namely, the scattering can occur only at a point in which one ξ particle is annihilated and another created. To recapitulate our method, the procedure is as follows:

(a) Compute the S-matrix element in a completely covariant fashion omitting all propagators which are on the mass shell. Denote this part of the result symbolically by

$$\langle p',(N-1)k,k'|S'-1|p,Nk\rangle.$$

(b) Evaluate

$$\langle p',(N-1)k|\hat{U}'^{\dagger}(0,+\infty)\hat{U}'(0,+\infty)|p',(N-1)k\rangle$$

and

$$\langle p,(N-1)k|\hat{U}'^{\dagger}(0,+\infty)\hat{U}'(0,+\infty)|p,(N-1)k\rangle$$

by the method of (B12). *In doing so omit again propagators with vanishing denominators.*

(c) Combining (a) and (b)

$$\langle p',(N-1)k,k'|S-1|p,Nk\rangle=\frac{\langle p',(N-1)k',|S'-1|p,Nk\rangle}{(\langle p',(N-1)k|\hat{U}'^{\dagger}(0,+\infty)\hat{U}'(0,+\infty)|p',(N-1)k\rangle)^{1/2}}$$
$$\times\frac{1}{(\langle p,(N-1)k|\hat{U}'^{\dagger}(0,+\infty)\hat{U}'(0,+\infty)|p,(N-1)k\rangle)^{1/2}}. \quad \text{(B13)}$$

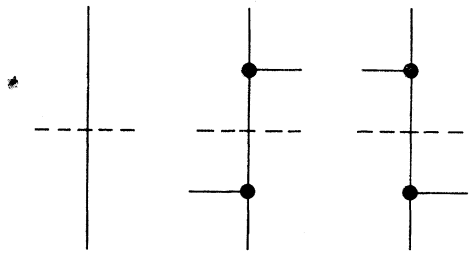

FIG. 20. χ-particle-factored forward scattering graphs through order $e^2\rho$.

In terms of Feynman graphs the procedure can be stated simply. One first computes the S-matrix element of interest, omitting contribution from graphs containing on-mass-shell propagators (i.e., in the language of the text, omitting graphs containing x_0 factors). Then the normalizations of the initial and final states are computed by the method of Eq. (B12). For example, consider the renormalization factor through order ρe^2. One draws the graphs through this order (shown in Fig. 20) with the straight dotted line to indicate that the χ-particle vertex has been factored out. By collecting the factors from the propagators and the remaining vertices one obtains

$$1+2\frac{e^2\rho}{2\omega}\left(\frac{p\cdot\epsilon}{p\cdot k}\right)^2+0(e^4\rho^2),$$

which agrees with the expansion of $\{J_0(2a)\}^{-2}$.